Front. Optoelectron. 2016, 9(1): 60–70
DOI 10.1007/s12200-016-0567-6

RESEARCH ARTICLE

Effect of electron-withdrawing groups in conjugated bridges: molecular engineering of organic sensitizers for dye-sensitized solar cells

Jie SHI[1,2], Zhaofei CHAI[1], Runli TANG[1], Huiyang LI[1], Hongwei HAN[3], Tianyou PENG[1], Qianqian LI (✉)[1], Zhen LI (✉)[1]

1 Department of Chemistry, Hubei Key Lab on Organic and Polymeric Opto-Electronic Materials, Wuhan University, Wuhan 430072, China
2 Hubei Key Laboratory of Oilcrops Lipid Chemistry and Nutrition, Oil Crops Research Institute, Chinese Academy of Agricultural Sciences, Wuhan 430062, China
3 Michael Grätzel Center for Mesoscopic Solar Cells, Wuhan National Laboratory for Optoelectronics, Huazhong University of Science and Technology, Wuhan 430074, China

Abstract Four organic sensitizers containing quinoxaline or benzoxadiazole as an auxiliary electron acceptor in conjugated bridge were synthesized and utilized for dye-sensitized solar cells (DSSCs). It was found that the incorporation of different electron-withdrawing moieties can affect the absorption spectra, electronic properties, the interfacial interactions and then the overall conversion efficiencies significantly. Therefore, the appropriate selection of the auxiliary acceptor was important to optimize the photovoltaic performance of solar cells. Among these sensitizers, **LI-44** based solar cell showed the best photovoltaic performance: a shortcircuit photocurrent density (J_{sc}) of 13.90 mA/cm^2, an open-circuit photovoltage (V_{oc}) of 0.66 V, and a fill factor (*FF*) of 0.66, corresponding to an overall conversion efficiency of 6.10% under standard global AM 1.5 solar light conditions.

Keywords dye-sensitized solar cells (DSSCs), auxiliary electron acceptor, quinoxaline, benzoxadiazole

1 Introduction

Dye sensitized solar cells (DSSCs) are considered as potential candidates for renewable-energy systems since the first report by Grätzel's group in 1991 [1,2]. As a key component in DSSCs, the photosensitizer is of unfailing research focus and substantial efforts have been devoted to the exploration of organic dyes in the past decade, primarily owing to the abundance of raw materials and flexibility of molecular design [3]. However, most of the organic dyes, commonly modeled on the donor-(π-spacer)-acceptor (D-π-A) configuration, have relatively narrow absorption spectra, which always located in the region of shorter wavelength. To expand the absorption spectra for harvesting more sunlight, a new kind of organic sensitizers with "D-A′-π-A" configuration has been reported, which incorporated additional electron-withdrawing groups (A′), such as benzothiadiazole [4–6], benzotriazole [7], quinoxaline [8–12], isoindigo [13], and so on, into the π bridge [14–17]. These A′ moieties usually displayed several advantages: 1) efficiently facilitating the electron transfer from the donor to the acceptor; 2) directly reducing the energy gap of organic dyes, leading to the broad light-harvesting region; 3) greatly improving the photostabilities. For these advantages, many organic sensitizers with "D-A′-π-A" configuration have been reported and most of them displayed excellent photovoltaic performance [16,18]. However, it does not work well for all the D-A′-π-A sensitizers [19,20]. Sometimes, the addition of the electron-withdrawing moieties may be adverse to the enhancement of conversion efficiency of the corresponding DSSCs, even worse than that of traditional ones, which was due to many factors, such as the lifetime of excited state, dipole moment, injection driving force, the charge recombination process, and so on [21]. Thus, the selection of the electron-withdrawing moieties was very important, since the different electronic properties and stereochemical structures of A′ moieties in the conjugated bridge affected the photovoltaic performance in a large degree. With the aim to investigate the function of the electron-withdrawing moieties in the conjugated bridge in detail, in this work, two heterocyclic rings with unlike electron-withdrawing

Received November 30, 2015; accepted January 4, 2016

E-mails: qianqian-alinda@163.com, lizhen@whu.edu.cn

abilities, quinoxaline and benzoxadiazole units, were incorporated into the conjugated bridge to exploit novel organic sensitizers with D-A′-π-A configurations. Normally, triphenylamine and 9-hexylcarbazole acted as the electron donor (D), and cyanoacetic acid as the electron acceptor (A) (Fig. 1) [22]. Moreover, the alkyl chains were substituted to the thiophene ring to inhibit the possible intermolecular aggregation and charge recombination [23]. Among the four organic sensitizers, DSSC based on **LI-44** with quinoxaline as the A′ moiety, showed the best light to electricity conversion efficiency of 6.10% (shortcircuit photocurrent density (J_{sc}) = 13.90 mA/cm^2, open-circuit photovoltage (V_{oc}) = 0.66 V, fill factor (*FF*) = 0.66) without any co-adsorbent. Herein, we report their syntheses, structural characterization, electrochemical properties, theoretical calculations, and photovoltaic performance.

2 Experimental

2.1 Materials

Tetrahydrofuran (THF) and toluene were dried over and distilled from K-Na alloy under an atmosphere of dry nitrogen. *N, N*-dimethylformamide (DMF) was dried over and distilled from CaH_2 under an atmosphere of dry nitrogen. 1, 2-dichloromethane was dried over and distilled from phosphorus pentoxide. Phosphorus oxychloride was freshly distilled before use. All reagents were purchased and used as received. 3,6-dibromobenzene-1,2-diamine [24] and 4,7-dibromobenzo[c] [1,2,5]oxadiazole [25] were prepared according to literature procedures.

2.2 Instrumentation

^{1}H and ^{13}C nuclear magnetic resonance (NMR) spectroscopy study was conducted with a Varian Mercury 300 spectrometer using tetramethylsilane (TMS; $\delta = 0$ ppm[1)]) as internal standard. Ultraviolet-visible (UV-vis) spectra were obtained using a Shimadzu UV-2550 spectrometer. Cyclic voltammograms were carried out on a CHI 660 voltammetric analyzer at room temperature in nitrogen-purged anhydrous dichloromethane with tetrabutylammonium hexafluorophosphate ($TBAPF_6$) as the supporting electrolyte at a scanning rate of 100 mV/s. A platinum disk and a Ag/AgCl electrode were used as the working electrode and quasi-reference electrode, respectively. The ferrocene/ferrocenium redox couple was used for potential calibration. Elemental analyses were performed by a 73 CARLOERBA-1106 micro-elemental analyzer. Electron impact mass spectra (EI-MS) were recorded with a Finnigan PRACE mass spectrometer.

2.3 Synthesis

5,8-Dibromo-2,3-dimethylquinoxaline (1). To the solution of 3,6-dibromobenzene-1,2-diamine (1.33 g, 5.0 mmol) in 60 mL ethanol, diacetyl (0.65 g, 7.5 mmol) was added slowly and the resultant solution was stirred at 60°C overnight. The mixture was extracted with chloroform and then washed with water for several times. The organic phase was dried over anhydrous Na_2SO_4. Removal of the solvent gave a crude product, which was further purified by silica-gel column chromatography to obtain **1** as a light yellow oil (1.18 g, 75%). ^{1}H NMR ($CDCl_3$, 300 MHz) δ (ppm): 7.84 (d, J = 2.4 Hz, 2H, ArH), 2.84 (s, 6H, -CH_3).

5,8-Bis(4-hexylthiophen-2-yl)-2,3-dimethylquinoxaline (2). To a solution of compound **1** (1.18 g, 3.75 mmol) and tributyl(4-hexylthiophen-2-yl)stannane (4.28 g, 9.37 mmol) in toluene (30 mL), was added $Pd(PPh_3)_4$ (0.012 g, 0.01 mmol) under an atmosphere of nitrogen. After refluxing for 12 h, the mixture was cooled to room

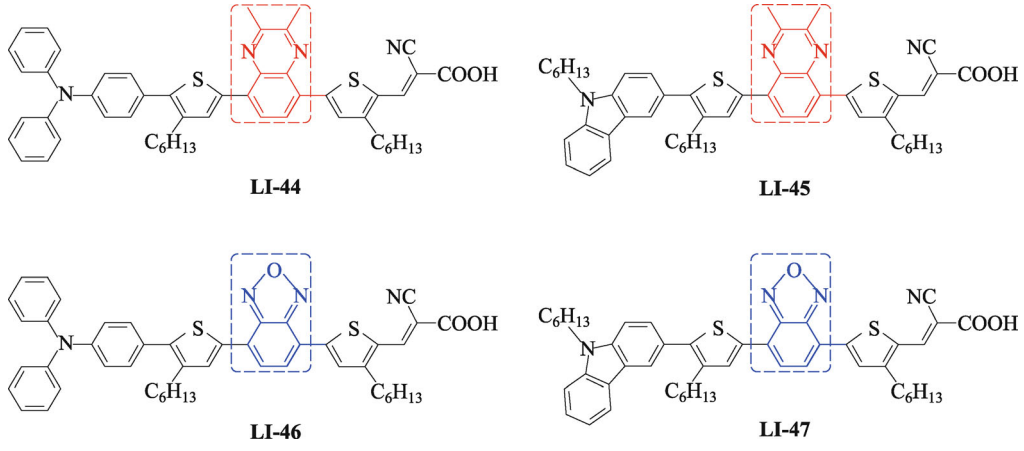

Fig. 1 Chemical structures of the four organic sensitizers

1) 1 ppm = 1×10^{-6}

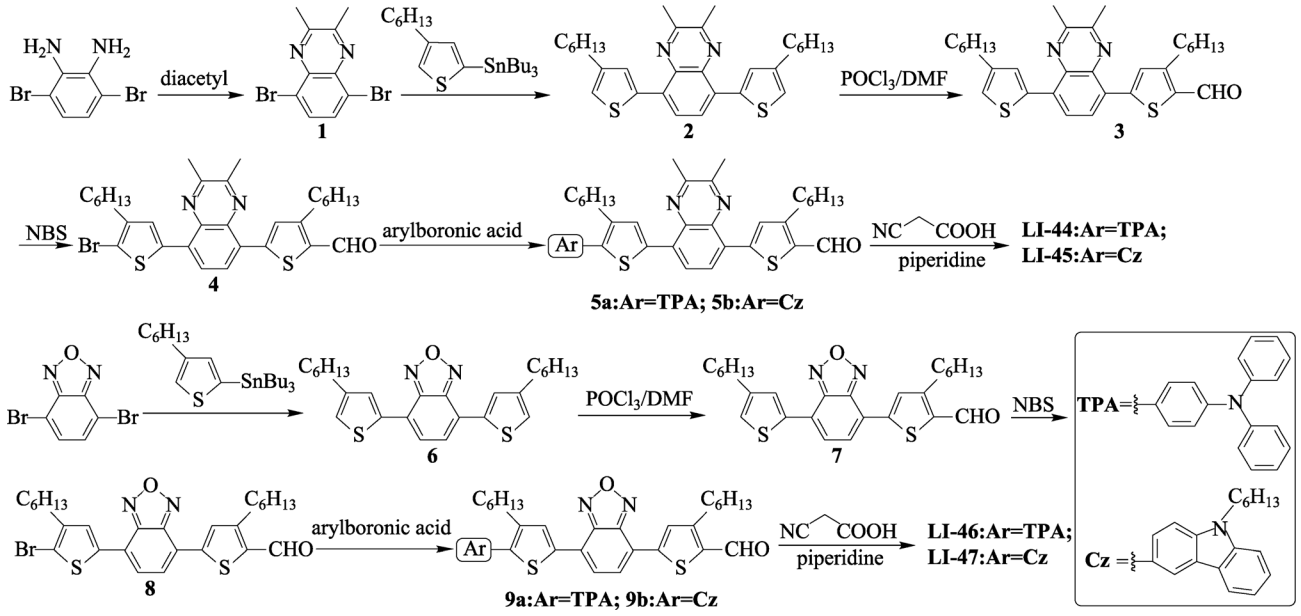

Scheme 1 Synthetic routes of the four organic sensitizers

temperature and then poured into water, the organic layer was extracted by CH_2Cl_2 and dried over anhydrous Na_2SO_4. The crude product was purified through a silica gel chromatography column to give **2** as a yellow oil (1.67 g, 90%). ^{1}H NMR ($CDCl_3$, 300 MHz) δ (ppm): 7.96 (br, 2H, ArH), 7.66 (s, 2H, ArH), 7.06 (s, 2H, ArH), 2.78 (s, 6H, -CH_3), 2.65 (t, J = 6.9 Hz, 4H, -CH_2-), 1.69-1.66(m, 4H, -CH_2-), 1.34 (br, 12H, -CH_2-), 0.90 (br, 6H, -CH_3).

3-Hexyl-5-(8-(4-hexylthiophen-2-yl)-2,3-dimethylquinoxalin-5-yl)thiophene-2-carbaldehyde (3). DMF (0.51 g, 7.0 mmol) was added to freshly distilled $POCl_3$ (0.54 g, 3.5 mmol) under an atmosphere of dry nitrogen at 0°C, and the resultant solution was stirred until its complete conversion into a glassy solid. After the addition of compound **2** (1.23 g, 2.5 mmol) in 1, 2-dichloroethane (30 mL) dropwise, the mixture was stirred at room temperature overnight, then poured into an aqueous solution of sodium acetate (1 M[1)], 200 mL), and stirred for another 2 h. The mixture was extracted with chloroform for several times, the organic fractions were combined and dried over anhydrous Na_2SO_4. After removing the solvent under vacuum, the crude product was purified through a silica gel chromatography column to give **3** as a red oil (0.98 g, 76%). ^{1}H NMR ($CDCl_3$, 300 MHz) δ (ppm): 10.10 (s, 1H, -CHO), 8.04 (d, J = 8.1 Hz, 1H, ArH), 7.98 (d, J = 8.1 Hz, 1H, ArH), 7.71 (s, 1H, ArH), 7.65 (s, 1H, ArH), 7.12 (s, 1H, ArH), 3.00 (t, J = 7.2 Hz, 2H, -CH_2-), 2.80 (s, 3H, -CH_3), 2.79 (s, 3H, -CH_3), 2.68 (t, J = 7.5 Hz, 2H, -CH_2-), 1.77-1.65 (m, 4H, -CH_2-), 1.43-1.34 (m, 12H, -CH_2-), 0.90 (br, 6H, -CH_3).

5-(8-(5-Bromo-4-hexylthiophen-2-yl)-2,3-dimethylquinoxalin-5-yl)-3-hexylthiophene-2-carbalde hyde (4). To a solution of compound **3** (0.78 g, 1.5 mmol) in $CHCl_3$ (15 mL) was added *N*-bromosuccinimide (0.27 g, 1.5 mmol). This mixture was stirred for 10 h in the absence of light at room temperature and then removed the solvent under vacuum. The crude product was purified through a silica gel chromatography column to give **4** as a red solid (0.80 g, 89%). ^{1}H NMR ($CDCl_3$, 300 MHz) δ (ppm): 10.10 (s, 1H, -CHO), 8.05 (d, J = 7.8 Hz, 1H, ArH), 8.00 (br, 1H, ArH), 7.67 (s, 1H, ArH), 7.50 (s, 1H, ArH), 3.01 (t, J = 6.6 Hz, 2H, -CH_2-), 2.80 (br, 6H, -CH_3), 2.63 (t, J = 7.5 Hz, 2H, -CH_2-), 1.75-1.58 (m, 4H, -CH_2-), 1.35 (br, 12H, -CH_2-), 0.91 (br, 6H, -CH_3).

General synthesis of 5. A mixture of **4** (597.0 mg, 1.0 mmol), 4-(Diphenyl amino)phenylboronic acid or 9-hexyl-9H-carbazol-3-ylboronic acid (2.0 mmol), sodium carbonate (2.12 g, 20.0 mmol), and $Pd(PPh_3)_4$ (0.012 g, 0.01 mmol) was carefully degassed and charged with nitrogen, and then dissolved in the solvent system of THF (monomer concentration about 0.025 M)/water (2:1 in volume). The reaction was stirred for 24 h at 80°C. After cooled to room temperature, the organic layer was separated, and evaporated to dryness. The crude product was purified by column chromatography over silica gel to give **5**.

5-(8-(5-(4-(Diphenylamino)phenyl)-4-hexylthiophen-2-yl)-2,3-dimethylquinoxalin-5-yl)-3-hexyl thiophene-2-carbaldehyde (5a). Red solid. 0.53 g. Yield: 69%. ^{1}H NMR ($CDCl_3$, 300 MHz) δ (ppm): 10.10 (s, 1H, -CHO), 8.09 (d, J = 6.0 Hz, 1H, ArH), 8.05 (d, J = 6.0 Hz, 1H, ArH), 7.75 (s, 1H, ArH), 7.67 (s, 1H, ArH), 7.31 (br, 2H, ArH), 7.29-7.27 (m, 4H, ArH), 7.17-7.04 (m, 8H, ArH),

1) 1 M = 1 mol/L

3.02 (t, J = 6.0 Hz, 2H, -CH_2-), 2.83 (br, 6H, -CH_3), 2.72 (t, J = 6.0 Hz, 2H, -CH_2-), 1.76-1.68 (m, 4H, -CH_2-), 1.39-1.26 (m, 12H, -CH_2-), 0.90-0.81 (m, 6H, -CH_3).

3-Hexyl-5-(8-(4-hexyl-5-(9-hexyl-9H-carbazol-3-yl) thiophen-2-yl)-2,3-dimethylquinoxalin-5-yl) thiophene-2-carbaldehyde (5b). Red solid. 0.57 g. Yield: 76%. ^{1}H NMR ($CDCl_3$, 300 MHz) δ (ppm): 10.10 (s, 1H, -CHO), 8.24 (br, 1H, ArH), 8.12 (br, 1H, ArH), 8.04 (br, 2H, ArH), 7.81 (br, 2H, ArH), 7.66 (s, 1H, ArH), 7.47 (s, 1H, ArH), 7.44 (br, 1H, ArH), 7.34 (s, 1H, ArH), 7.25 (br, 1H, ArH), 4.32 (br, 2H, -CH_2-), 2.98 (br, 2H, -CH_2-), 2.79 (br, 6H, -CH_3), 2.73 (br, 2H, -CH_2-), 1.90-1.66 (m, 6H, -CH_2-), 1.33 (br, 18H, -CH_2-), 0.88 (br, 9H, -CH_3).

4,7-Bis(4-hexylthiophen-2-yl)benzo[c] [1,2,5**]oxadiazole (6).** The syntheses of **6** was followed the same procedure as that of compound **2** using appropriate compounds. Red oil. 1.49 g. Yield: 87%. ^{1}H NMR ($CDCl_3$, 300 MHz) δ (ppm): 7.96 (s, 2H, ArH), 7.56 (br, 2H, ArH), 7.03 (s, 2H, ArH), 2.68 (t, J = 7.5 Hz, 4H, -CH_2-), 1.71-1.61 (m, 4H, -CH_2-), 1.39-1.32 (m, 12H, -CH_2-), 0.95-0.90 (m, 6H, -CH_3).

3-Hexyl-5-(7-(4-hexylthiophen-2-yl)benzo[c] [1,2,5**] oxadiazol-4-yl)thiophene-2-carbaldehyde (7).** The syntheses of **7** was followed the same procedure as that of compound **3** using appropriate compounds. Red solid. 1.02 g. Yield: 85%. ^{1}H NMR ($CDCl_3$, 300 MHz) δ (ppm): 10.11 (s, 1H, -CHO), 8.06 (s, 1H, ArH), 8.04 (s, 1H, ArH), 7.72 (br, 1H, ArH), 7.62 (br, 1H, ArH), 7.09 (s, 1H, ArH), 3.03 (t, J = 6.0 Hz, 2H, -CH_2-), 3.03 (t, J = 6.3 Hz, 2H, -CH_2-), 1.85-1.71 (m, 4H, -CH_2-), 1.34 (br, 12H, -CH_2-), 0.92-0.89 (m, 6H, -CH_3).

5-(7-(5-Bromo-4-hexylthiophen-2-yl)benzo[c] [1,2,5**] oxadiazol-4-yl)-3-hexylthiophene-2-carbalde hyde (8).** The syntheses of **8** was followed the same procedure as that of compound **4** using appropriate compounds. Red solid. 0.74 g. Yield: 81%. ^{1}H NMR ($CDCl_3$, 300 MHz) δ (ppm): 10.10 (s, 1H, -CHO), 8.05 (s, 1H, ArH), 7.87 (s, 1H, ArH), 7.72 (d, J = 7.2 Hz, 1H, ArH), 7.51 (d, J = 7.8 Hz, 1H, ArH), 3.02 (t, J = 7.5 Hz, 2H, -CH_2-), 2.63 (t, J = 7.8 Hz, 2H, -CH_2-), 1.76-1.63 (m, 4H, -CH_2-), 1.39-1.25 (m, 12H, -CH_2-), 0.90 (br, 6H, -CH_3).

General synthesis of 9. The syntheses of **9** was followed the same procedure as that of compound **5** using appropriate compounds.

5-(7-(5-(4-(Diphenylamino)phenyl)-4-hexylthiophen-2-yl)benzo[c] [1,2,5**]oxadiazol-4-yl)-3-hexyl thiophene-2-carbaldehyde (9a).** Red solid. 0.53 g. Yield: 73%. ^{1}H NMR ($CDCl_3$, 300 MHz) δ (ppm): 10.10 (s, 1H, -CHO), 8.08 (s, 1H, ArH), 8.05 (s, 1H, ArH), 7.73 (d, J = 7.2 Hz, 1H, ArH), 7.58 (d, J = 7.6 Hz, 1H, ArH), 7.37-7.29 (m, 6H, ArH), 7.17- 7.04 (m, 8H, ArH), 3.01 (t, J = 7.2 Hz, 2H, -CH_2-), 2.74 (t, J = 8.4 Hz, 2H, -CH_2-), 1.76-1.71 (m, 4H, -CH_2-), 1.31 (br, 12H, -CH_2-), 0.89 (br, 6H, -CH_3).

3-Hexyl-5-(7-(4-hexyl-5-(9-hexyl-9H-carbazol-3-yl) thiophen-2-yl)benzo[c] [1,2,5**]oxadiazol-4-yl) thiophene-2-carbaldehyde (9b).** Red solid. 0.49 g. Yield: 77%. ^{1}H NMR ($CDCl_3$, 300 MHz) δ (ppm): 10.10 (s, 1H, -CHO), 8.22 (br, 1H, ArH), 8.13 (br, 1H, ArH), 8.11 (s, 1H, ArH), 8.06 (s, 1H, ArH), 7.75 (d, J = 7.2 Hz, 1H, ArH), 7.63-7.59 (m, 2H, ArH), 7.51-7.43 (m, 4H, ArH), 4.34 (t, J = 7.2 Hz, 2H, -CH_2-), 3.01 (t, J = 8.1 Hz, 2H, -CH_2-), 2.79 (t, J = 7.8 Hz, 2H, -CH_2-), 1.91-1.69 (m, 6H, -CH_2-), 1.33-1.25 (m, 18H, -CH_2-), 0.90-0.85 (m, 9H, -CH_3).

General synthesis of organic dyes. A mixture of **5** or **9** (0.25 mmol) and cyanoacetic acid (85 mg, 1.0 mmol) were vacuum-dried, then MeCN (15.0 mL), THF (5.0 mL) and piperidine (10 μL) were added. The solution was refluxed for 8 h. After the solution was cooled, the organic layer was removed under vacuum. The product was purified by column chromatography.

2-Cyano-3-(5-(8-(5-(4-(diphenylamino)phenyl)-4-hexylthiophen-2-yl)-2,3-dimethyl-2,3-dihydro quinoxalin-5-yl)-3-hexylthiophen-2-yl)acrylic acid (LI-44). Red solid. 0.14 g. Yield: 68%. ^{1}H NMR (DMSO-d_6, 300 MHz) δ (ppm): 8.29-8.24 (m, 2H, ArH), 8.16 (br, 1H, -CH =), 7.91 (br, 1H, ArH), 7.89 (br, 1H, ArH), 7.39-7.29 (m, 6H, ArH), 7.09-6.99 (m, 8H, ArH), 2.73 (br, 6H,-CH_3), 2.67 (br, 4H, -CH_2-), 1.61 (br, 4H, -CH_2-), 1.27-1.24 (m, 12H, -CH_2-), 0.84-0.82 (m, 6H, -CH_3). ^{13}C NMR (DMSO-d_6, 75 MHz) δ (ppm): 165.16, 156.62, 156.47, 153.19, 147.57, 147.09, 146.18, 142.14, 137.71, 136.57, 135.58, 133.39, 131.75, 130.23, 130.07, 128.86, 127.49, 126.28, 124.89, 124.00, 123.33, 117.87, 31.69, 31.12, 30.88, 29.27, 28.86, 28.51, 22.75, 14.59. MS (EI), m/z [M]: 828.38, (calcd: 828.35). Anal. Calcd for: $C_{52}H_{52}N_4O_2S_2$: C, 75.33; H, 6.32; N, 6.76. Found: C, 75.08; H, 6.80; N, 6.73.

2-Cyano-3-(3-hexyl-5-(8-(4-hexyl-5-(9-hexyl-9H-carbazol-3-yl)thiophen-2-yl)-2,3-dimethyl quinoxalin-5-yl) thiophen-2-yl)acrylic acid (LI-45). Red solid. 0.16 g. Yield: 74%. ^{1}H NMR (DMSO-d_6, 300 MHz) δ (ppm): 8.34-8.29 (m, 2H, ArH), 8.24-8.18 (m, 3H, ArH and -CH =), 7.96 (br, 2H, ArH), 7.67-7.47 (m, 4H, ArH), 7.17 (br, 1H, ArH), 4.25 (t, J = 6.6 Hz, 2H, -CH_2-), 2.41 (t, J = 7.5 Hz, 2H, -CH_2-), 2.13 (t, J = 7.8 Hz, 2H, -CH_2-), 1.77 (br, 2H, -CH_2-), 1.64 (br, 4H, -CH_2-), 1.28-1.20 (m, 18H, -CH_2-), 0.84-0.75 (m, 9H, -CH_3). ^{13}C NMR (DMSO-d_6, 75 MHz) δ (ppm): 160.12, 152.68, 145.55, 143.55, 142.31, 141.03, 139.94, 137.65, 136.65, 135.79, 133.67, 130.12, 129.86, 129.54, 127.37, 126.45, 125.65, 122.94, 122.71, 120.84, 119.44, 119.05, 109.59, 103.03, 31.79, 31.36, 29.36, 29.18, 26.98, 22.83, 14.50. MS (EI), m/z [M]: 834.67, (calcd: 834.40). Anal. Calcd for: $C_{52}H_{60}N_4O_2S_2$: C, 74.78; H, 7.00; N, 6.71. Found: C, 74.31; H, 6.93; N, 6.34.

2-Cyano-3-(5-(7-(5-(4-(diphenylamino)phenyl)-4-hexylthiophen-2-yl)benzo[c] [1,2,5**]oxadiazol-4-yl) − 3-hexylthiophen-2-yl)acrylic acid (LI-46).** Black solid. 0.17 g. Yield: 84%. ^{1}H NMR (DMSO-d_6, 300 MHz) δ (ppm): 8.19 (s, 1H, -CH =), 7.94 (s, 1H, ArH), 7.89 (s, 1H, ArH), 7.86 (br, 1H, ArH), 7.73 (d, J = 7.2 Hz, 1H, ArH), 7.35-7.31 (m, 6H, ArH), 7.12-6.97 (m, 8H, ArH), 2.77 (br, 3H, -CH_3), 2.63 (br, 3H, -CH_3), 2.41 (t, J = 7.2 Hz, 2H,

-CH_2-), 2.13 (t, J = 8.1 Hz, 2H, -CH_2-), 1.60 (br, 4H, -CH_2-), 1.30-1.25 (m, 12H, -CH_2-), 0.85-0.83 (m, 6H, -CH_3). ^{13}C NMR (DMSO-d_6, 75 MHz) δ (ppm): 160.13, 151.19, 145.51, 145.19, 138.82, 137.76, 132.37, 130.08, 129.57, 128.02, 127.97, 127.71, 127.04, 125.07, 122.96, 121.79, 120.86, 120.40, 117.13, 31.56, 30.93, 30.68, 29.20, 29.05, 28.91, 27.88, 22.61, 22.23, 14.33. MS (EI), m/z [M]: 790.21, (calcd: 790.30). Anal. Calcd for: $C_{48}H_{46}N_4O_3S_2$: C, 72.88; H, 5.86; N, 7.08. Found: C, 72.49; H, 6.04; N, 6.79.

2-Cyano-3-(3-hexyl-5-(7-(4-hexyl-5-(9-hexyl-9H-carbazol-3-yl)thiophen-2-yl)benzo[c] [1,2,5] oxadiazol-4-yl)thiophen-2-yl)acrylic acid (LI-47). Black solid. 0.14 g. Yield: 74%. ^{1}H NMR (DMSO-d_6, 300 MHz) δ (ppm): Red solid. 0.14 g. Yield: 69%. 8.17-8.11 (m, 3H, ArH and -CH =), 7.91 (s, 1H, ArH), 7.83 (s, 1H, ArH), 7.77 (d, J = 7.5 Hz, 1H, ArH), 7.67 (d, J = 6.6 Hz, 1H, ArH), 7.55 (br, 2H, ArH), 7.48 (s, 1H, ArH), 7.45 (s, 1H, ArH), 7.18 (d, J = 7.2 Hz, 1H, ArH), 4.34 (br, 2H, -CH_2-), 2.75 (br, 2H, -CH_2-), 2.65 (br, 2H, -CH_2-), 1.74 (br, 2H, -CH_2-), 1.60 (br, 4H, -CH_2-), 1.29-1.83 (m, 18H, -CH_2-), 0.85-0.74 (m, 9H, -CH_3). ^{13}C NMR (DMSO-d_6, 75 MHz) δ (ppm): 161.21, 152.61, 147.36, 142.14, 140.78, 139.86, 139.47, 134.36, 131.96, 130.04, 127.10, 126.79, 126.33, 124.22, 122.76, 122.32, 120.61, 119.29, 109.43, 102.30, 31.44, 30.99, 30.71, 29.15, 28.88, 26.69, 22.52, 14.19. MS (EI), m/z [M]: 796.42, (calcd: 796.35). Anal. Calcd for: $C_{48}H_{52}N_4O_3S_2$: C, 72.33; H, 6.58; N, 7.03. Found: C, 72.09; H, 6.75; N, 6.98.

2.4 Device fabrication

A layer of *ca.* 2 μm TiO_2 (TPP-3, Heptachroma, China) was coated on the fluorine-tin-oxide (FTO) conducting glass by screen printing and then dried for 6 min at 125°C. This procedure was repeated 6 times (*ca.* 12 μm) and finally coated by a layer (*ca.* 4 μm) of TiO_2 paste (TPP-200, Heptachroma, China) as the scattering layer. The TiO_2 electrodes were gradually heated under an air flow at 450°C for 30 min. The sintered film was further treated with 0.2 M $TiCl_4$ aqueous solution at room temperature for 12 h, then washed with water and ethanol, and annealed at 450°C for 30 min. After the film was cooled to 80°C, it was immersed in a sensitizer bath (3×10^{-4} M) in CH_2Cl_2 solution and maintained in the dark for 24 h at room temperature. The electrode was then rinsed with CH_2Cl_2 and dried. The size of the TiO_2 electrodes was 0.238 cm^2. To prepare the counter electrode, the Pt catalyst was deposited on cleaned FTO glass by coating with a drop of H_2PtCl_6 solution (0.02 M 2-propanol solution) with heat treatment at 400°C for 15 min. A hole (0.8 mm diameter) was drilled on the counter electrode using a drill-press. The perforated sheet was cleaned with ultrasound in an ethanol bath for 10 min. For the assembly of DSSCs, the sensitizer-covered TiO_2 electrode and Pt-counter electrode were assembled into a sandwich type cell and sealed with a hot-melt gasket of 25 μm thickness made of the ionomer Surlyn 1702 (DuPont). The electrolyte (DHS-Z23, Heptachroma, China) was introduced into the cell via vacuum backfilling from the hole in the back of the counter electrode. Finally, the hole was sealed using a piece of aluminum foil tape.

2.5 Photovoltaic properties measurements

The DSSC was illuminated by light with energy of a 100 mW/cm^2 from 300 W AM 1.5G simulated sunlight (2 × 2 beam, w/6258 lamp, Newport, USA). The light intensity was determined using a SRC-1000-TC-QZ-N reference monocrystalline silicon cell system (Oriel, USA), which was calibrated by National Renewable Energy Laboratory, A2LA accreditation certificate 2236.01. The current-voltage (J-V) curves for the fabricated DSSCs were collected by using CHI618 electrochemical analyzer (CH Instruments). Cell active area was tested with a mask of 0.16 cm^2. The electrochemical impedance spectra (EIS) measurements were carried out with applying bias of the open circuit voltage (V_{oc}) under the conditions and recorded over a frequency range from 0.05 to 105 Hz with ac amplitude of 10 mV. Incident photon-to-current conversion efficiency (IPCE) was recorded on a DC Power Meter (Model 2931-C, Newport Co.) under irradiation of a 300 W xenon lamp light source with a motorized monochromator (Oriel). The xenon lamp was powered by an Arc Lamp Power Supply (Model 69920, Newport Co.).

3 Results and discussion

3.1 Synthesis

These sensitizers were synthesized using the synthetic protocol described in Scheme 1. Through a Stille coupling with tributyl(4-hexylthiophen-2-yl)stannane and bromine-substituted heterocyclic rings bearing electron-withdrawing properties, conjugated bridge of the organic dyes (compound **2** and **6**) were formed. Followed by the Vilsmeier reaction, the corresponding monoaldehyde-substituted derivatives **3** and **7** were synthesized and then the bromide reactions occurred with NBS, converting them to **4** and **8**, respectively. The electron donor unit, triphenylamine or 9-hexylcarbazole, was attached to the conjugated bridge by Suzuki coupling to obtain the intermediates **5a**-**b** and **9a**-**b**. Finally, the obtained intermediates converted to the corresponding sensitizers by Knoevenagel condensation with cyanoacetic acid in the presence of piperidine. These sensitizers were well soluble in common organic solvents (i.e., acetone, CH_2Cl_2, $CHCl_3$, DMF, DMSO and THF). The structure and purity of the sensitizers were confirmed by ^{1}H NMR, ^{13}C NMR, ESI-MS and elemental analysis.

3.2 Absorption spectra

The absorption spectra of sensitizers in dichloromethane solution were displayed in Fig. 2, and the corresponding data was presented in Table 1. All the sensitizers exhibited two absorption bands, the absorption bands shorter than 450 nm were assigned to a π–π* transition, while the absorption bands at longer wavelength corresponded to the internal charge transfer (ICT) [26,27]. Dye **LI-44** and **LI-45**, which consisted of the same electron-withdrawing group (quinoxaline), showed the similar maximum wavelength (λ_{max}) of the absorption spectra, indicating that the similar electron-donating ability of triphenylamine and 9-hexylcarbazole moieties. But the molar extinction coefficient (ε) of **LI-44** with triphenylamine as the electron donor was much higher than that of **LI-45** bearing 9-hexylcarbazole as donor group. The similar phenomena were also observed in the case of **LI-46** and **LI-47**. However, in comparison with the λ_{max}s of **LI-44** and **LI-45**, those of **LI-46** and **LI-47** were red-shifted over 30 nm, indicating the stronger electron-withdrawing ability of benzoxadiazole unit. And the absorption onset of **LI-47** was up to 700 nm, showing the broad light-harvesting region.

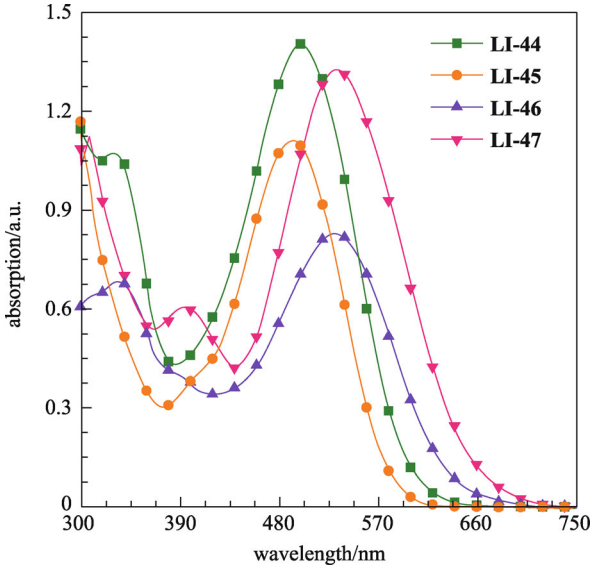

Fig. 2 UV-vis spectra of the four organic sensitizers in CH_2Cl_2

The absorption spectra of organic sensitizers anchoring onto a transparent nanocrystalline TiO_2 film (6 μm) were shown in Fig. 3. And the similar λ_{max}s of the four dyes with that in solutions indicated the well-organized arrangement of the dyes and possibly no severe dye aggregates on the TiO_2 film [28]. Accordingly, **LI-46** and **LI-47** bearing benzoxadiazole in the conjugated bridge exhibited broader absorption region, which may favor the light harvesting of the solar cells.

3.3 Electrochemical properties

To evaluate the possibilities of electron injection from the excited state of the sensitizers to conduction band (CB) of semiconductor and the regeneration of the oxidized dyes, the oxidation potentials of the sensitizers were determined from cyclic voltammograms, and the related data were collected in Table 1. Generally, the oxidation potential vs normal hydrogen electrode (NHE) (E_{ox}) corresponded to the highest occupied molecular orbital (HOMO), while the reduction potential vs NHE (E_{red}), which corresponded to the lowest unoccupied molecular orbital (LUMO), could be calculated from $E_{ox} - E_{0\text{-}0}$. The first onset oxidation potentials of the four dyes, which were ascribed to oxidation of the electron donors, were 0.94, 1.19, 0.95 and 1.20 V, respectively. The similar potentials of **LI-44** and **LI-46** were due to the same electron donor of the two dyes (triphenylamine), also the same with the case of **LI-45** and **LI-47** bearing carbazole as the electron donor. And the higher HOMO levels of **LI-44** and **LI-46** demonstrated the stronger electron donating ability of triphenylamine than that of carbazole unit. Since an over-potential of 0.2 V was sufficiently enough for the electron injection to TiO_2 film, all the dyes were energetically permitted from the calculations of driving force. The reduction potentials of **LI-44**, **LI-45**, **LI-46** and **LI-47** were calculated to be −1.15, −0.95, −1.00 and −0.72 V, respectively. From **LI-44** to **LI-45**, the lower LUMO level was due to the change of electron donor from triphenylamine to carbazole, and the lower LUMO level of **LI-46** than that of **LI-44** was on account of the stronger electron-withdrawing ability of benzoxadiazole in comparison with that of

Table 1 Absorbance and electrochemical properties of the sensitizers

dye	$\lambda_{max}{}^{a}$/nm	ε^{a}/($M^{-1}\cdot cm^{-1}$)	$\lambda_{max}{}^{b}$/nm	$E_{0\text{-}0}{}^{c}$/eV	$E_{ox}{}^{d}$/V vs NHE	$E_{red}{}^{e}$/V vs NHE
LI-44	499	46700	490	2.09	0.94	− 1.15
LI-45	492	37000	488	2.14	1.19	− 0.95
LI-46	530	27700	528	1.95	0.95	− 1.00
LI-47	532	44000	531	1.91	1.20	− 0.72

[a] Absorption spectra of dyes measured in CH_2Cl_2 with the concentration of 3×10^{-5} mol/L. [b] Absorption spectra of dyes adsorbed on the surface of TiO_2. [c] The bandgap, $E_{0\text{-}0}$ was derived from the observed optical edge. [d] E_{ox} were measured in CH_2Cl_2 with $(n\text{-}C_4H_9)_4NPF_6$ as electrolyte (scanning rate, 100 mV/s; working electrode and counter electrode, Pt wires; reference electrode, Ag/AgCl). The oxidation potential (E_{ox}) referenced to calibrated Ag/AgCl was converted to the NHE reference scale: $E_{ox} = E_{ox}{}^{on} + 0.2$ V. [e] E_{red} was calculated from $E_{ox} - E_{0\text{-}0}$

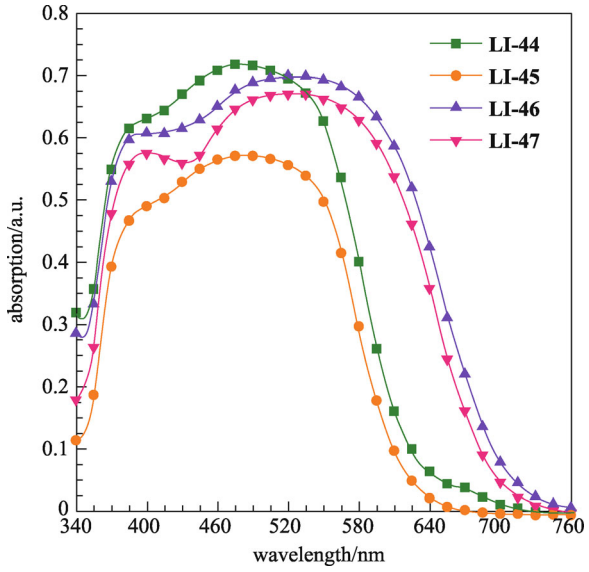

Fig. 3 UV-vis spectra of the four organic sensitizers on TiO_2 films

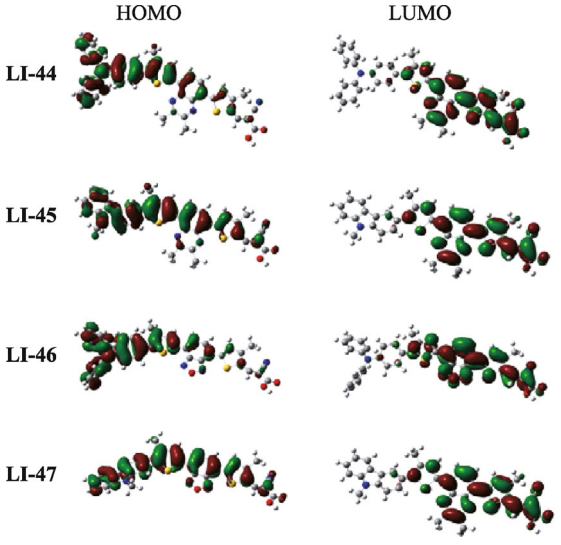

Fig. 4 Frontier orbitals of the sensitizers optimized at the B3LYP/6-31G* level

quinoxaline moiety. Thus, **LI-47**, bearing carbazole as the electron donor and benzoxadiazole as the auxiliary electron acceptor (A′) in the conjugated bridge, exhibited the lowest LUMO level (−0.72 V), which may not be sufficient enough to inject electrons into the TiO_2 films.

3.4 Theoretical approach

To gain further insight in the correlation between structure and the physical properties as well as the device performance, quantum chemistry computation was conducted. The geometries of sensitizers were optimized using time-depending DFT (TD-DFT) calculations with Gaussian 09 program, and the B3LYP exchange-correlation functional and a 6-31G* basis set were used to analyze the structures of the sensitizers [29]. As depicted in Fig. 4, all the π-conjugated segments maintained relatively good coplanar conformation. And the HOMOs of the four dyes were distributed along the π-system of the donor and the conjugated bridge, while the LUMOs were almost delocalized across the entire A′-π-A system. However, in comparison with the HOMOs of **LI-44** and **LI-46**, that of **LI-45** and **LI-47** were distributed and extended to the whole molecule. This could be beneficial to the overlap of HOMO and LUMO orbitals, resulting in the efficient intramolecular charge transfer. However, on the other hand, it may cause more charge recombination, resulting in the decrease of conversion efficiency.

3.5 Photovoltaic performance of DSSCs

The photovoltaic characteristics of these sensitizers were obtained with a sandwich cell using the commercial redox electrolyte (DHS-Z23, Heptachroma, China). The action spectra of IPCE for DSSCs based on the four sensitizers were showed in Fig. 5, the light could be converted to photocurrent efficiently in the range of 400 – 700 nm. And the highest IPCE values of 78% at 478 nm, 62% at 472 nm, 26% at 518 nm, and 30% at 517 nm were achieved for the DSSCs based on **LI-44**, **LI-45**, **LI-46**, and **LI-47**, respectively. The relatively boarder IPCE curves of **LI-46** and **LI-47**, which were in good accordance with the absorption spectra of dye-loading TiO_2 films, were attributed to the stronger electron-withdrawing properties of the benzoxadiazole unit. However, the lower IPCE values of the two dyes indicated the possible electron trapper effect and charge recombination in the corresponding DSSCs.

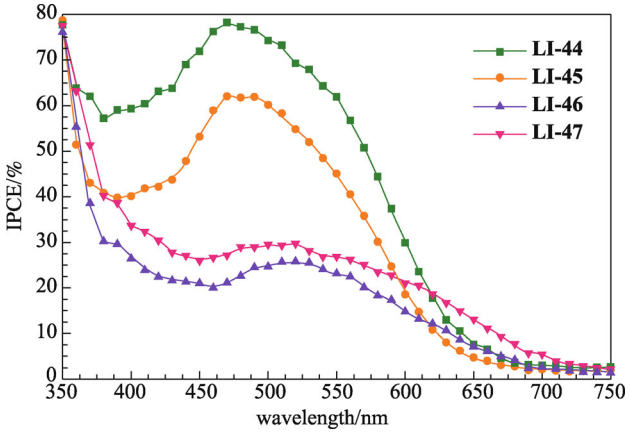

Fig. 5 Spectra of monochrmatic IPCE for DSSCs based on these sensitizers

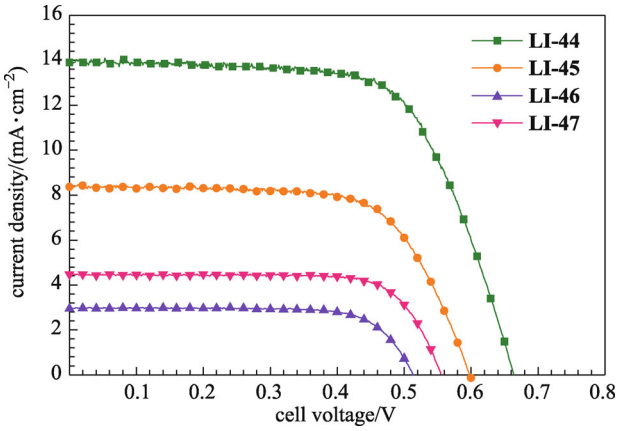

Fig. 6 Current density-voltage characteristics obtained with a nanocrystalline TiO_2 film supported on FTO conducting glass and derivatized with monolayer of sensitizers

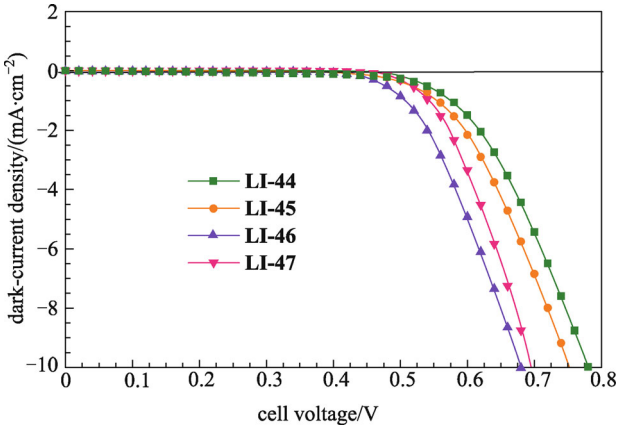

Fig. 7 Dark-current density-potential curves of DSSCs based on these sensitizers

The *J-V* curves of the DSSCs sensitized by the four dyes were shown in Fig. 6, and the detailed photovoltaic parameters were summarized in Table 2. Under standard global AM 1.5 solar conditions, the **LI-44** sensitized cell exhibited the best photovoltaic performance: J_{sc} of 13.90 mA/cm^2, V_{oc} of 0.66 V, and *FF* of 0.66, corresponding to an overall conversion efficiency (η) of 6.10%. When the electron donor of **LI-44** was replaced to carbazole unit, **LI-45**-sensitized solar cell showed the lower conversion efficiency of 3.37%, mainly due to the decreased J_{sc} of 8.31 mA/cm^2. It may be caused by the lower driving force for the electron injection and the possible charge recombination. Once the auxiliary electron acceptor (A′) of **LI-44** and **LI-45** was changed to benzoxadiazole moiety, the decreased conversion efficiencies were obtained from the solar cells based on **LI-46** and **LI-47**. In spite that they exhibited broad light-harvesting response extended to the 750 nm, the J_{sc}s of the corresponding solar cells were 2.93 and 4.43 mA/cm^2, respectively, which much lower than that of **LI-44** and **LI-45**. With the aim to investigate the possible influence factors, we tested the dark currents of DSSCs based on the four dyes, which were shown in Fig. 7. Obviously, the higher dark currents of DSSCs based on **LI-46** and **LI-47** bearing benzoxadiazole in the conjugated bridge, indicated that the stronger electron-withdrawing ability of benzoxadiazole may cause the severe charge recombination, leading to the lower J_{sc} values and reduced conversion efficiencies.

Besides, many organic sensitizers usually aggregated on the TiO_2 surface via molecular stacking, leading to the self-quenching and reducing electron injection into TiO_2. Generally, chenodeoxycholic acid (CDCA) is used as a coadsorbent to dissociate the π-stacked sensitizer aggregations and improve the electron-injection yield, thus affording a higher J_{sc} value [30]. In consideration of this, the photovoltaic performances of the DSSCs with and without CDCA were investigated and the corresponding

Table 2 Performance data of DSSCs based on the four sensitizers [a]

sensitizer	CDCA [b]	J_{sc}/(mA·cm^{-2})	V_{oc}/V	*FF*	η/%
LI-44	none	13.90	0.66	0.66	6.10
	1 mM	11.90	0.65	0.68	5.35
	5 mM	10.93	0.64	0.62	4.35
LI-45	none	8.31	0.60	0.68	3.37
	1 mM	9.43	0.61	0.71	4.03
	5 mM	8.56	0.63	0.68	3.67
LI-46	none	2.93	0.51	0.75	1.13
	1 mM	3.10	0.52	0.73	1.18
	5 mM	2.89	0.52	0.68	1.02
LI-47	none	4.43	0.55	0.75	1.84
	1 mM	3.58	0.56	0.77	1.56
	5 mM	1.73	0.56	0.72	0.70

[a] Illumination: 100 mW/cm^2 simulated AM 1.5 G solar light. [b] Expose to relative CDCA solution for 6 h before the dye bath

data were summarized in Table 2. It was worth to note that the addition of CDCA did not optimize the photovoltaic performance in our case, even decreased the power conversion efficiencies. A possible explanation was that the dye aggregation in these solar cells were not severe, which may be due to the multi hydrophobic chains in the conjugated bridges to weaken the intermolecular interactions. Thus, the coadsorption of CDCA was not essential for these dyes. On the other hand, the coadsorption of CDCA reduced the amount of sensitizers adsorbed on the TiO_2 surface, resulting in the loss of active light harvesting, then leading to the lower conversion efficiencies [31].

3.6 Electrochemical impedance spectroscopy

To gain more insight into the DSSCs properties, EIS was performed to investigate the effect on charge recombination, transport and collection [32,33]. The Nyquist plots of DSSCs with different sensitizers in the dark and under a forward bias of −0.7 V were shown in Fig. 8(a). The charge recombination resistance (R_{rec}) at the TiO_2 surface deduced by fitting curves from the range of intermediate frequency using a Z-view software, and the R_{rec} values of **LI-44**–**LI-47** were calculated to be 185.4, 85.9, 10.7 and 20.9 Ω, respectively. The higher electron recombination resistance indicated more effective suppression of the back reactions, which caused by the injected electrons in the TiO_2 film together with I_3^- in the electrolyte. With the similar trend in dark currents of DSSCs, the benzoxadiazole with stronger electron-withdrawing property in **LI-46** and **LI-47** may led more charge recombination, resulting in the decrease of J_{sc} and V_{oc}. Figure 8(b) demonstrated the EIS Nyquist plots for DSSCs, upon illumination under open-circuit conditions (100 mW/cm^2). The lower electron transport resistance (R_{et}) can assist electron collection and improve the cell efficiency. The fitted R_{et} values of **LI-44**–**LI-47** were calculated to be 24.6, 34.4, 65.5 and 46.4 Ω, respectively, which also indicated the influence of different auxiliary electron acceptors in the conjugated bridge on the photovoltaic performance. In comparison with benzoxadiazole, the incorporation of quinoxaline moiety may be better for the electron injection, transport and collection in the corresponding solar cells. Another important parameter for DSSCs, electron lifetime (τ), could be calculated from the peak in middle frequency of the Bode phase plot, and the electron lifetime under different series of bias voltage were revealed in Fig. 9. At a fixed bias voltage, the electron lifetime of **LI-44** was significantly longer than that of the other three dyes. The photoelectrons possessing longer lifetimes had more chances of entering the external circuit and contributing to the photoelectric conversion efficiency, and the results of the electron lifetime were well consistent with those parameters in photovoltaic characteristics, giving an explanation of the different V_{oc}s yielded by DSSCs based on the four sensitizers.

4 Conclusions

In summary, a series of metal-free organic sensitizers with D-A′-π-A configurations have been designed and synthesized, in which quninoxaline or benzoxadiazole moiety was incorporated into the conjugated bridge as the auxiliary electron acceptor (A′) to extend the absorption spectra and broaden the light-harvesting region. Interestingly, the introduction of the two moieties with different electron-withdrawing abilities gave big difference in the photovoltaic performance of the corresponding solar cells. The benzoxadiazole moiety, with the stronger electron-withdrawing property, can expand the absorption spectra of the related dyes in solution and TiO_2 film more efficiently, leading to the broader IPCE curves. But it can also act as the electron trapper, which was adverse to the electron injection and resulted in the severe charge recombination, leading to the decreased conversion efficiencies of DSSCs based on **LI-46** and **LI-47**. And the addition of quninoxaline unit with mild electron-withdrawing property can gave a good balance of the

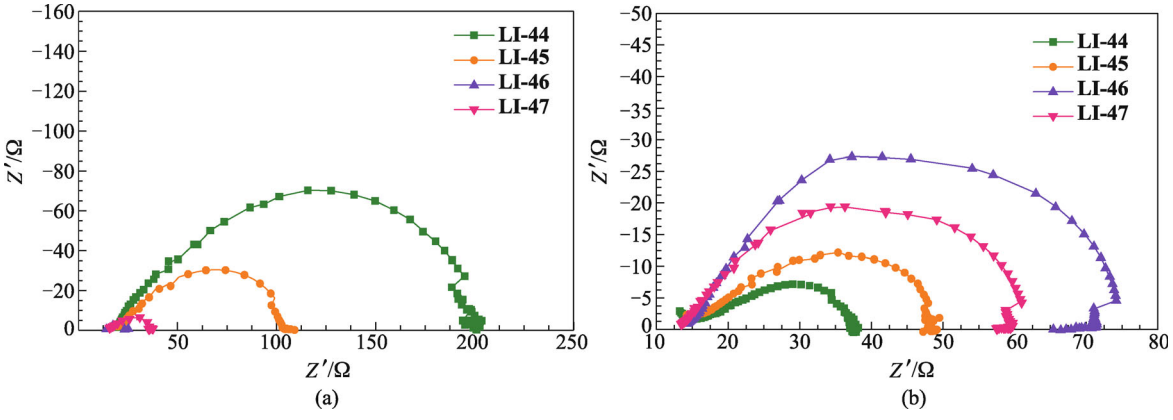

Fig. 8 EIS for DSSCs based on the sensitizers. (a) Nyquist plots in the dark; (b) Nyquist plots under illumination

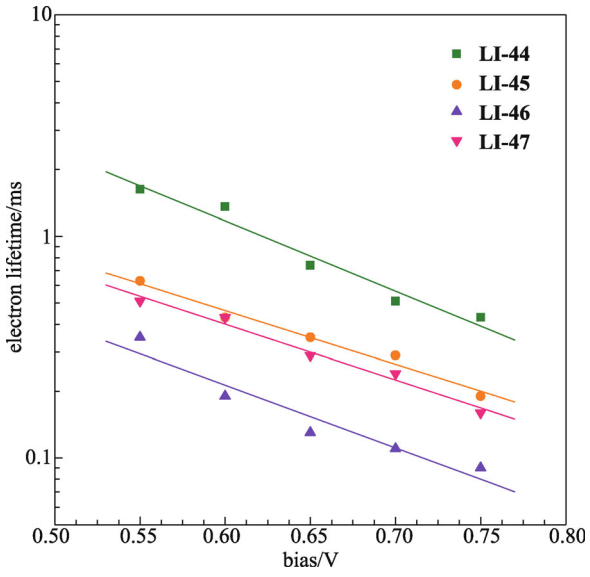

Fig. 9 Electron lifetime fitted from impedance spectra under a series of applied potentials

above two effect on the photovoltaic performance, and the solar cell based on **LI-44** showed the best light to electricity conversion efficiency of 6.10% (J_{sc} = 13.90 mA/cm^2, V_{oc} = 0.66 V, FF = 0.66) without any co-adsorbent.

Acknowledgements We are grateful to the National Natural Science Foundation of China (Grant Nos. 21372003 and 21325416), Hubei Province Natural Science Foundation of China (No. 2014CFB698) for financial support.

References

1. O'Regan B, Grätzel M. A low-cost, high-efficiency solar cell based on dye-sensitized colloidal TiO_2 films. Nature, 1991, 353(6346): 737–740
2. Hagfeldt A, Boschloo G, Sun L, Kloo L, Pettersson H. Dye-sensitized solar cells. Chemical Reviews, 2010, 110(11): 6595–6663
3. Hardin B E, Snaith H J, McGehee M D. The renaissance of dye-sensitized solar cells. Nature Photonics, 2012, 6(3): 162–169
4. Joly D, Pellejà L, Narbey S, Oswald F, Chiron J, Clifford J N, Palomares E, Demadrille R. A robust organic dye for dye sensitized solar cells based on iodine/iodide electrolytes combining high efficiency and outstanding stability. Scientific Reports, 2014, 4: 4033
5. Joly D, Pellejà L, Narbey S, Oswald F, Meyer T, Kervella Y, Maldivi P, Clifford J N, Palomares E, Demadrille R. Metal-free organic sensitizers with narrow absorption in the visible for solar cells exceeding 10% efficiency. Energy & Environmental Science, 2015, 8(7): 2010–2018
6. Kang X, Zhang J, O'Neil D, Rojas A J, Chen W, Szymanski P, Marder S R, El-Sayed M A. Effect of molecular structure perturbations on the performance of the D-A–π-A dye sensitized solar cells. Chemistry of Materials, 2014, 26(15): 4486–4493
7. Cui Y, Wu Y, Lu X, Zhang X, Zhou G, Miapeh F B, Zhu W, Wang Z S. Incorporating benzotriazole moiety to construct D-A–π-A organic sensitizers for solar cells: significant enhancement of open-circuit photovoltage with long alkyl group. Chemistry of Materials, 2011, 23(19): 4394–4401
8. Pei K, Wu Y, Islam A, Zhang Q, Han L, Tian H, Zhu W. Constructing high-efficiency D-A-π-A-featured solar cell sensitizers: a promising building block of 2,3-diphenylquinoxaline for antiaggregation and photostability. ACS Applied Materials & Interfaces, 2013, 5(11): 4986–4995
9. Lu X, Feng Q, Lan T, Zhou G, Wang Z S. Molecular engineering of quinoxaline-based organic sensitizers for highly efficient and stable dye-sensitized solar cells. Chemistry of Materials, 2012, 24(16): 3179–3187
10. Shi J, Chen J, Chai Z, Wang H, Tang R, Fan K, Wu M, Han H, Qin J, Peng T, Li Q, Li Z. High performance organic sensitizers based on 11,12-bis(hexyloxy) dibenzo[a,c]phenazine for dye-sensitized solar cells. Journal of Materials Chemistry, 2012, 22(36): 18830–18838
11. Yang J, Ganesan P, Teuscher J, Moehl T, Kim Y J, Yi C, Comte P, Pei K, Holcombe T W, Nazeeruddin M K, Hua J, Zakeeruddin S M, Tian H, Grätzel M. Influence of the donor size in D-π-A organic dyes for dye-sensitized solar cells. Journal of the American Chemical Society, 2014, 136(15): 5722–5730
12. Li X, Hu Y, Sanchez-Molina I, Zhou Y, Yu F, Haque S A, Wu W, Hua J, Tian H, Robertson N. Insight into quinoxaline containing D-π-A dyes for dye-sensitized solar cells with cobalt and iodine based electrolytes: the effect of π-bridge on the HOMO energy level and photovoltaic performance. Journal of Materials Chemistry A, Materials for Energy and Sustainability, 2015, 3(43): 21733–21743
13. Ying W, Guo F, Li J, Zhang Q, Wu W, Tian H, Hua J. Series of new D-A-π-A organic broadly absorbing sensitizers containing isoindigo unit for highly efficient dye-sensitized solar cells. ACS Applied Materials & Interfaces, 2012, 4(8): 4215–4224
14. Zhu W, Wu Y, Wang S, Li W, Li X, Chen J, Wang Z, Tian H. Organic D-A-π-A solar cell sensitizers with improved stability and spectral response. Advanced Functional Materials, 2011, 21(4): 756–763
15. Wu Y, Marszalek M, Zakeeruddin S M, Zhang Q, Tian H, Grätzel M, Zhu W. High-conversion-efficiency organic dye-sensitized solar cells: molecular engineering on D-A-π-A featured organic indoline dyes. Energy & Environmental Science, 2012, 5(8): 8261–8272
16. Wu Y, Zhu W. Organic sensitizers from D-π-A to D-A-π-A: effect of the internal electron-withdrawing units on molecular absorption, energy levels and photovoltaic performances. Chemical Society Reviews, 2013, 42(5): 2039–2058
17. Eom Y K, Choi I T, Kang S H, Lee J, Kim J, Ju M J, Kim H K. Thieno[3, 2-*b*] benzothiophene derivative as a new π-bridge unit in D-π-A structural organic sensitizers with over 10.47% efficiency for dye-sensitized solar cells. Advanced Energy Materials, 2015, 5(15): 1500300
18. Wu Y, Zhu W H, Zakeeruddin S M, Grätzel M. Insight into D-A-π-A structured sensitizers: a promising route to highly efficient and stable dye-sensitized solar cells. ACS Applied Materials & Interfaces, 2015, 7(18): 9307–9318

19. Chai Z, Wu M, Fang M, Wan S, Xu T, Tang R, Xie Y, Mei A, Han H, Li Q, Li Z. Similar or totally different: the adjustment of the twist conformation through minor structural modification, and dramatically improved performance for dye-sensitized solar cell. Advanced Energy Materials, 2015, 5(18): 1500846
20. Haid S, Marszalek M, Mishra A, Wielopolski M, Teuscher J, Moser J E, Humphry-Baker R, Zakeeruddin S M, Grätzel M, Bäuerle P. Significant improvement of dye-sensitized solar cell performance by small structural modification in π-conjugated donor-acceptor dyes. Advanced Functional Materials, 2012, 22(6): 1291–1302
21. Yen Y S, Chou H H, Chen Y C, Hsu C Y, Lin J T. Recent developments in molecule-based organic materials for dye-sensitized solar cells. Journal of Materials Chemistry, 2012, 22(18): 8734–8747
22. Liang M, Chen J. Arylamine organic dyes for dye-sensitized solar cells. Chemical Society Reviews, 2013, 42(8): 3453–3488
23. Koumura N, Wang Z S, Mori S, Miyashita M, Suzuki E, Hara K. Alkyl-functionalized organic dyes for efficient molecular photovoltaics. Journal of the American Chemical Society, 2006, 128(44): 14256–14257
24. Yamamoto T, Sugiyama K, Kushida T, Inoue T, Kanbara T. Preparation of new electron-accepting π-conjugated polyquinoxalines. Chemical and electrochemical reduction, electrically conducting properties, and use in light-emitting diodes. Journal of the American Chemical Society, 1996, 118(16): 3930–3937
25. Blouin N, Michaud A, Gendron D, Wakim S, Blair E, Neagu-Plesu R, Belletête M, Durocher G, Tao Y, Leclerc M. Toward a rational design of poly(2,7-carbazole) derivatives for solar cells. Journal of the American Chemical Society, 2008, 130(2): 732–742
26. Li H, Yang Y, Hou Y, Tang R, Duan T, Chen J, Wang H, Han H, Peng T, Chen X, Li Q, Li Z. Organic sensitizers featuring 9,10-diaryl-substituted anthracene unit. ACS Sustainable Chemistry & Engineering, 2014, 2(7): 1776–1784
27. Li Q, Shi J, Li H, Li S, Zhong C, Guo F, Peng M, Hua J, Qin J, Li Z. Novel pyrrole-based dyes for dye-sensitized solar cells: from rod-shape to "H" type. Journal of Materials Chemistry, 2012, 22(14): 6689–6696
28. Li H, Hou Y, Yang Y, Tang R, Chen J, Wang H, Han H, Peng T, Li Q, Li Z. Attempt to improve the performance of pyrrole-containing dyes in dye sensitized solar cells by adjusting isolation groups. ACS Applied Materials & Interfaces, 2013, 5(23): 12469–12477
29. Frisch G W T M J, Schlegel H B, Scuseria G E, Robb M A, Cheeseman J R, Scalmani G, Barone V, Mennucci B, Petersson G A, Nakatsuji H, Caricato M, Li X, Hratchian H P, Izmaylov A F, Bloino J, Zheng G, Sonnenberg J L, Hada M, Ehara M, Toyota K, Fukuda R, Hasegawa J, Ishida M, Nakajima T, Honda Y, Kitao O, Nakai H, Vreven T, Montgomery J A Jr, Peralta J E, Ogliaro F, Bearpark M, Heyd J J, Brothers E, Kudin K N, Staroverov V N, Kobayashi R, Normand J, Raghavachari K, Rendell A,Burant J C, Iyengar S S, Tomasi J, Cossi M, Rega N, Millam J M, Klene M, Knox J E, Cross J B, Bakken V, Adamo C, Jaramillo J, Gomperts R, Stratmann R E, Yazyev O, Austin A J, Cammi R, Pomelli C, Ochterski J W, Martin R L, Morokuma K, Zakrzewski V G, Voth G A, Salvador P, Dannenberg J J, Dapprich S, Daniels A D, Farkas Ö, Foresman J B, Ortiz J V, Cioslowski J, Fox D J. Gaussian, Inc., Wallingford CT. 2009
30. Salvatori P, Marotta G, Cinti A, Anselmi C, Mosconi E, De Angelis F. Supramolecular interactions of chenodeoxycholic acid increase the efficiency of dye-sensitized solar cells based on a cobalt electrolyte. Journal of Physical Chemistry C, 2013, 117(8): 3874–3887
31. Tang J, Hua J, Wu W, Li J, Jin Z, Long Y, Tian H. New starburst sensitizer with carbazole antennas for efficient and stable dye-sensitized solar cells. Energy & Environmental Science, 2010, 3 (11): 1736–1745
32. Wang Q, Moser J E, Grätzel M. Electrochemical impedance spectroscopic analysis of dye-sensitized solar cells. Journal of Physical Chemistry B, 2005, 109(31): 14945–14953
33. Adachi M, Sakamoto M, Jiu J, Ogata Y, Isoda S. Determination of parameters of electron transport in dye-sensitized solar cells using electrochemical impedance spectroscopy. Journal of Physical Chemistry B, 2006, 110(28): 13872–13880

Qianqian Li received her B.Sc. degree from Hubei University, China in 2004, and then obtained her Ph.D. degree at Wuhan University in 2009. She is now an associate professor at Wuhan University, and her research interests are in the design and synthesis of new electric and optical functional materials.